Range Cell Migration Processing Loss in Automotive Radar

Adrien Grivey, Kevin Cinglant, Fabrice Comblet, Ali Khenchaf

Range Cell Migration Processing Loss in Automotive Radar

Adrien Grivey[$#], Kevin Cinglant[#], Fabrice Comblet[$], Ali Khenchaf[$]
[$]Lab-STICC CNRS UMR 6285, ENSTA Bretagne, France
[#]ZF Autocruise, France
adrien.grivey@ensta-bretagne.org

***Abstract* — Frequency Modulated Continuous Wave (FMCW) automotive radar using stretch-processing usually relies on a fast-chirp signal model which assumes range and Doppler decoupling between fast and slow-time dimensions. To achieve high range and speed resolutions, a large bandwidth and a long coherent processing interval are used. However, if multiple range resolution cells are crossed during the integration duration, fast-chirp signal model assumption becomes inaccurate, resulting in misfocusing in both fast and slow-time dimensions. This misfocusing leads to the misestimation of target parameters and a loss of coherent integration. In this paper, Range Cell Migration (RCM) processing loss is studied and illustrated using a FMCW signal model. Furthermore, a windowing in both dimensions is proposed to mitigate this loss.**

***Keywords* — Range cell migration, FMCW radar, processing loss, windowing**

I. Introduction

Automotive radar has become a commodity sensor, widely used to develop Advanced Driving Assistance Systems (ADAS) functions such as adaptative cruise control, lane change assist or autonomous driving [1]. FMCW modulation scheme is a classic waveform for range and speed estimations in automotive radar. Stretch processing (or dechirping) technique [2] is used instead of matched filtering for pulse compression. The emitted linearly frequency modulated (LFM) waveform sweeps a wide bandwidth to reach a fine range resolution with pulse compression. Stretch processing permits tractable sampling frequency for automotive radar while preserving the matched filter range resolution (meter to centimeter), at the expense of a limited range span. A coherent FMCW pulse-train produces a Coherent Processing Interval (CPI), allowing speed to be retrieved by Doppler processing. Fast-chirp (or rapid chirp) scheme allows to derive a simplified but effective signal model where range and Doppler information are decoupled in two frequencies lying in two separate dimensions (see Fig. 1) [3].

Wide chirp bandwidth provides finer range resolution, though causes range walk during long CPI for high-speed targets. This range cell migration (RCM) spreads the pulse compressed signal energy across multiple range bins, therefore leading to a loss of coherent processing gain [4], [5]. Signal-processing based corrections have been studied in the literature, for example, [4] and [6] independently proposed a chirp z-transform. Slow-time modulation schemes have been proposed to compensate pulse-to-pulse RCM without signal processing efforts [7]. Without compensation method, the coherent processing loss due to RCM in an FMCW automotive context has not been detailed. It has only been approximated as the number of crossed range cells [5], [8]. Automotive radars are designed to meet stringent requirements, and RCM-induced loss may be an issue to achieve a given link budget. The goal of this paper is to quantify this loss and shows its dependency with the selected fast and slow-time windowing.

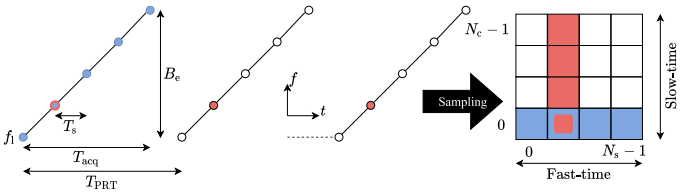

Fig. 1. FMCW pulse-train sampling and its fast and slow-time formatting

Apart from a conclusion and perspectives presented in part V, the rest of the paper is organized into three sections. The section II is dedicated to FMCW stretch-processing signal model. Section III focuses on the RCM effect and the coherent integration loss. Section IV presents the measured processing loss after fast and slow-time windowing, using an asymptotic expression and simulations.

II. Fast-chirp FMCW signal model

A pulse train of N_c LFM waveforms is emitted with a Pulse Repetition Time (PRT) of T_{PRT}. Individual chirps are emitted with an effective bandwidth B_e during chirp duration T_{acq}, with a start frequency f_l, as illustrated in Fig. 1. In stretch processing pulse compression [2], the received signal is demodulated by mixing it with the transmitted signal and the mixed signal is low pass filtered to keep only Intermediate Frequency (IF) component. Assuming IQ demodulation, the analogic IF signal of the signal reflected by a single scatterer target is:

$$s_a(t) = \sum_{m=0}^{N_c-1} A \exp\left(i\varphi_m(t)\right) w_{T_{acq}}(t - mT_{PRT}) \qquad (1)$$

where $\varphi_m(t) = 2\pi\left(\alpha\tau(t)t_m + f_l\tau(t)\right)$, $t \in [0, N_c T_{PRT}]$ is the absolute time, referenced since the beginning of the first pulse acquisition, and $t_m = t - mT_{PRT}$ is the time referenced since the beginning of the m-th pulse. A is the received amplitude of the signal, accounting for losses during propagation and reception. $\alpha = \frac{B_e}{T_{acq}}$ is the chirp rate, $w_{T_{acq}}$ is the windowing

function of duration T_{acq}, assumed to be rectangular at this point. $\tau(t)$ is the round-trip delay with respect to time. Let R_0 be the range of the point target at $t = 0$ and V_{r} its radial speed, assumed constant during the CPI. Substituting $\tau(t) = \frac{2(R_0+V_{\text{r}}t)}{c}$ in $\varphi_m(t)$ and keeping only the significant phase terms in an automotive radar context, the phase of the IF signal becomes:

$$\varphi_m(t) = 2\pi \left(f_{\text{IF},m} t_m + \frac{f_{\text{intra}}(t_m)}{2} t_m + \phi_{R_0} \right) \tag{2}$$

where $f_{\text{IF},m} = f_{\text{IF}} + f_{\text{inter}}[m]$, $f_{\text{IF}} = f_{\text{range}} - f_{\text{doppler}}$, $f_{\text{intra}}(t_m) = \frac{4\alpha V_{\text{r}}}{c} t_m$, and $f_{\text{inter}}[m] = \frac{2\alpha V_{\text{r}}}{c} m T_{\text{PRT}}$. The beat frequency $f_{\text{IF},m}$ contains both range and speed information in the frequency components $f_{\text{range}} = \frac{2\alpha R_0}{c}$ and $f_{\text{doppler}} = -\frac{2 f_{\text{l}} V_{\text{r}}}{c}$. The instantaneous frequency f_{intra} creates intra-pulse RCM, while the frequency f_{inter} creates inter-pulse RCM (see section III-A). The phase term $\phi_{R_0} = 2\pi \frac{2 f_{\text{l}} R_0}{c}$ is constant and can be discarded from the equations hereafter. In this section, we assume that intra and inter-pulse RCM are neglectable, so the Eq. (2) is:

$$\varphi_m(t) = 2\pi f_{\text{IF}} t_m \tag{3}$$

The N_{c} chirps of the pulse-train are captured, each with a sampling period $T_{\text{s}} = \frac{1}{f_{\text{s}}}$ so N_{s} samples are acquired. The sampled pulse sequence can be rearranged in a two-dimensional data array, so the sampled time $t = nT_{\text{s}} + mT_{\text{PRT}}$ is separated in the so-called fast-time $t_{\text{ft}} = nT_{\text{s}}$ and slow-time $t_{\text{st}} = mT_{\text{PRT}}$ (see Fig. 1):

$$s[n,m] = A \exp\left(i2\pi \left(f_{\text{IF}} n T_{\text{s}} - f_{\text{doppler}} m T_{\text{PRT}} \right)\right) \tag{4}$$

In fast-chirp FMCW [3], we assume that the chirp rate α is designed to sweep a wide bandwidth fast enough so the Doppler frequency term $f_{\text{doppler}} = \frac{-2 f_{\text{l}} V_{\text{r}}}{c}$ shifts the beat frequency less than the frequency resolution. Then, the frequency is assumed to be composed only by the range-related frequency f_{range} in such a way that $f_{\text{IF}} \approx f_{\text{range}}$. To estimate f_{range} and f_{doppler}, a 2D Discrete Fourier Transform (DFT) is applied along n and m indexed dimensions of the sampled signal given by Eq. (4):

$$\begin{aligned} S[N,M] &= \sum_{n=0}^{N_{\text{s}}-1} \sum_{n=0}^{N_{\text{c}}-1} s[n,m] \exp\left(-i2\pi \left(\frac{nN}{N_{\text{s}}} + \frac{mM}{N_{\text{c}}} \right)\right) \\ &= A\, D_{N_{\text{s}}} \left(\frac{N - N_{\text{r}}}{N_{\text{s}}} \right) D_{N_{\text{c}}} \left(\frac{M - M_{\text{d}}}{N_{\text{c}}} \right) \end{aligned} \tag{5}$$

where $D_N(x) = \exp\left(-i\pi(N-1)x\right) \frac{\sin(\pi N x)}{\sin(\pi x)}$ is the Dirichlet kernel [2], $N_{\text{r}} = f_{\text{range}} T_{\text{acq}}$ and $M_{\text{d}} = -f_{\text{doppler}} T_{\text{int}}$, with $T_{\text{int}} = N_{\text{c}} T_{\text{PRT}}$ is the CPI of the chirp sequence. A peak is centered at the reduced frequency bins N_{r} and M_{d} in discrete 2D spectrum, which position can be estimated by a peak search algorithm. The frequency resolution is defined as the null-to-null spacing in D_N. From Eq. (5), we can see that the frequency resolution is $\frac{1}{T_{\text{acq}}}$ in fast-time dimension and $\frac{1}{T_{\text{int}}}$ in the slow-time dimension. Then, range estimate has a resolution of $\Delta R = \frac{c}{2B_{\text{e}}}$ and the speed estimate has a resolution of $\Delta V_{\text{r}} = \frac{c}{2 f_{\text{l}} T_{\text{PRT}}}$.

Table 1. FMCW modulation parameters used in this study

Parameter	Notation	Value
Effective bandwidth	B_{e}	375 MHz
Sampling frequency / period	f_{s} / T_{s}	5 MHz / 0.2 µs
Start frequency	f_{l}	77 GHz
Pulse Repetition Time	T_{PRT}	100 µs
Number of samples per pulse	N_{s}	256
Number of pulses	N_{c}	256

III. Range cell migration signal model

A. Intra and inter-pulse range cell migrations

In this section, the FMCW signal model used for the RCM derivation is introduced.

Fast-chirp assumption made in the previous section to perform range-Doppler processing assumed that range and Doppler frequencies were uncoupled, so the estimated frequency in the fast-time dimension depended only on the range parameter. However, the beat frequency $f_{\text{IF}} = f_{\text{range}} - f_{\text{doppler}}$ measured during pulse processing is composed of both f_{range} and f_{doppler} [2]. An unambiguous speed measure should be considered during range estimation to avoid a bias proportional to speed. The spectrum shape is not affected by this bias, which only shifts the power spectrum peak along fast-time frequency dimension. Due to the target movement, the instantaneous beat frequency in Eq. (2) varies during the acquisition. The movement during one pulse acquisition, through the fast-time dependent instantaneous frequency f_{intra}, is named intra-pulse RCM, whereas the pulse-to-pulse movement through the slow-time dependent instantaneous frequency f_{inter} is named inter-pulse RCM [7].

First, intra-pulse RCM can be neglected in an automotive radar context. Indeed, using automotive radar parameters given in Table 1, the range resolution is $\Delta R = 40\,\text{cm}$ and the intra-pulse range migration is $V_{\text{r}} T_{\text{acq}} \approx 4\,\text{mm}$ at $V_{\text{r}} = 300\,\text{km·h}^{-1}$.

On the contrary, inter-pulse RCM effect can't be neglected in automotive scenario. Multiple range cells can be crossed during the full sequence acquisition. This case can be encountered on highways with two vehicles, both at $130\,\text{km·h}^{-1}$ but with opposite directions: for radar parameters in Table 1 the travelled distance is $V_{\text{r}} T_{\text{int}} \approx 1.8\,\text{m}$ at $V_{\text{r}} = 260\,\text{km·h}^{-1}$, while the range resolution is $\Delta R = 40\,\text{cm}$. From Eq. (2), the sampled signal model given by Eq. (4) is then reduced to the presence of inter-pulse RCM only:

$$\begin{aligned} &s_{\text{RCM}}[n,m] = \\ &\quad A \exp\left(i2\pi \left(\left(f_{\text{IF}} + f_{\text{inter}}[m] \right) n T_{\text{s}} - f_{\text{doppler}} m T_{\text{PRT}} \right)\right) \end{aligned} \tag{6}$$

B. Number of migrated range bins

With no RCM, the fast-time peak was initially centered around f_{IF} after fast-time processing in Eq. (5). Assuming only inter-pulse RCM, as in Eq. (6), the peak is incrementally shifted by the range variation $V_{\text{r}} m T_{\text{PRT}}$ at each new pulse m.

Therefore, the number of migrated range cells during the CPI is given by Eq. (7).

$$n_{\text{RCM}} = \frac{V_{\text{r}} T_{\text{int}}}{\Delta R} \tag{7}$$

By refactoring Eq. (6) with respect to pulse index m and performing a slow-time DFT only, it can be shown that the RCM also creates a Doppler cell migration. The number of migrated Doppler bins in slow-time frequency dimension is the same as the number of migrated range bins [5], [6], [8].

C. Coherent processing loss

The pulse-compressed and Doppler-processed fast-chirp signal model leads to focused energy in one range and speed bin in Eq. (5) when no RCM is involved. Windowing is a technique used to avoid spectral leakage, i.e. high sidelobes creating ghost targets. Sampled pulse train results in a two-dimensional signal (Eq. (6)), so two windows can be applied independently on the two dimensions:

$$s_w[n,m] = s[n,m]\, w_{\text{ft}}[n]\, w_{\text{st}}[m] \tag{8}$$

The 2D spectrum is obtained by the 2D DFT of the signal given by Eq. (8), denoted $S_w[N,M]$. The maximum peak power in the spectrum of a windowed pure tone signal is the coherent integration gain of the window [9]:

$$W[0]^2 = \left(\sum_{k=0}^{N_k-1} w(k) \right)^2 \tag{9}$$

where w is an arbitrary window and W its DFT:

$$W[K] = \sum_{k=0}^{N_k-1} w(k) \exp\left(-i2\pi \frac{kK}{N_k}\right) \tag{10}$$

Then, without RCM, the peak power of windowed fast-chirp signal model in Eq. (8) is $|S_w[N_{\text{r}}, M_{\text{d}}]|^2 = (AW_{\text{ft}}(0)W_{\text{st}}(0))^2$, e.g., when two rectangular windows are applied on the signal, the peak power in Eq. (5) is $(AN_{\text{s}}N_{\text{c}})^2$, which is the optimum coherent power gain that can be achieved [9]. The fast-chirp range-Doppler decoupling assumption led to an optimal coherent integration in both fast and slow-time dimensions. The 2D DFT is equivalent to a matched filter $h[n,m] = \exp\left(-i2\pi\left(\frac{nN_{\text{r}}}{N_{\text{s}}} + \frac{mM_{\text{d}}}{N_{\text{c}}}\right)\right)$ maximizing the output power at the matching frequency bins $(N_{\text{r}}, M_{\text{d}})$ [4].

When considering the RCM in signal model given by Eq. (6), the 2D spectrum is smeared through multiple range and speed resolution cells, so the energy is no more concentrated and the coherent peak power is decreased. The peak spreading after 2D DFT is illustrated in Fig. 2. Signal model given by Eq. (6) has been used to simulate a point target with (Fig. 2a) and without (Fig. 2b) RCM. Modulation parameters from Table 1 and target parameters $R_0 = 5\,\text{m}$ and $V_{\text{r}} = 55\,\text{m·s}^{-1}$ have been used in the simulation. The initial maximum peak power position is marked with a white cross in Fig. 2a and the detected maximum peak power after RCM is marked with a black cross in Fig. 2b. Besides the biases of the range and speed estimates, the peak power difference of $11.5\,\text{dB}$ exhibits

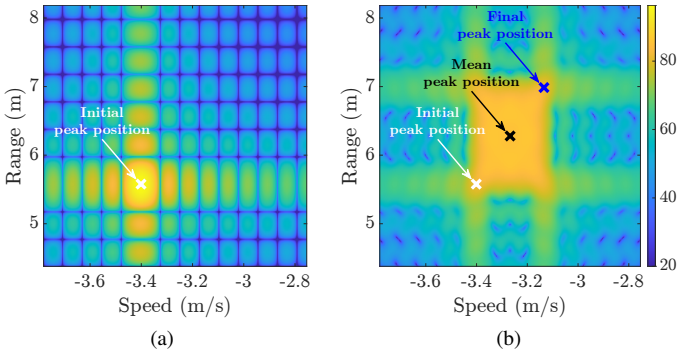

Fig. 2. Simulated range Doppler map using parameters in Table 1: (a) without RCM; (b) with RCM

the energy spreading. The matched filter without RCM $h[n,m]$ is no more the optimum matched filter in case of RCM. The matched filter accounting for the pulse-to-pulse range variation is $h_{\text{RCM}}[n,m] = h[n,m] \exp\left(-i2\pi \frac{\alpha n T_{\text{s}}}{f_{\text{l}}} \frac{mM_{\text{d}}}{N_{\text{c}}}\right)$ [4]. Hence, the output power of the 2D DFT with RCM is necessarily lower than the spectrum without RCM, leading to a loss of apparent SNR in the range-Doppler map:

$$\forall N, M, \quad |S_{\text{RCM}}[N,M]|^2 \leq (AW_{\text{ft}}[0]W_{\text{st}}[0])^2 \tag{11}$$

IV. Range Cell Migration Processing Loss Mitigation Using Windowing

A. Simulated processing loss

Finding an insightful expression of range-Doppler spectrum S_{RCM} to estimate processing loss due to RCM is complicated, especially with fast and slow-time windowing. To estimate this processing loss, the signal model in Eq. (6) is simulated with RCM, then the maximum peak power is estimated after range-Doppler processing and compared to the expected peak power for the applied windows. In other words, this is equivalent to compare the output powers of matched filters h and h_{RCM}. The detailed procedure is described below:

1) Generate discrete signal s_{RCM} as in Eq. (6) with a specified number of migrated range bins n_{RCM} (Eq. (7)), and apply fast and slow-time windows w_{ft} and w_{st} as in Eq. (8) to get windowed signal s_{w},
2) Compute S_{w}, the 2D DFT of s_{w},
3) Estimate the maximum peak power in 2D spectrum S_{w}:

$$P_{\text{peak}}^{\text{RCM}} = \max_{N,M} |S_w[N,M]|^2 \tag{12}$$

4) Compute processing loss by comparing the estimated peak power $P_{\text{peak}}^{\text{RCM}}$ with expected peak power without RCM $P_{\text{peak}}^{\text{expected}} = (AW_{\text{ft}}[0]W_{\text{st}}[0])^2$:

$$\text{PL} = \frac{P_{\text{peak}}^{\text{RCM}}}{P_{\text{peak}}^{\text{expected}}} \tag{13}$$

In step 2, the spectral precision is increased by zero-padding with 8 times more samples in both fast and slow-time dimensions than the number of samples and pulses indicated in Table 1. The scalloping loss [9] after zero-padding is less

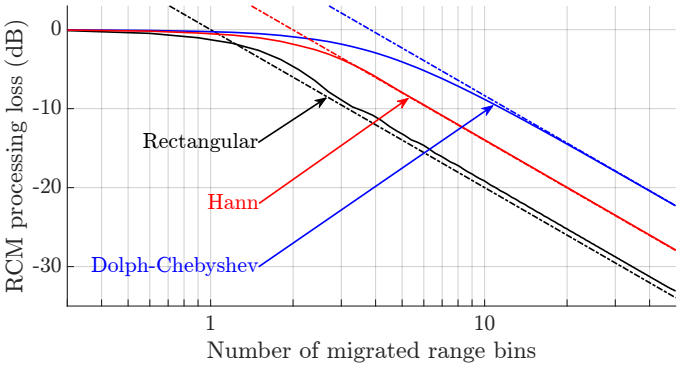

Fig. 3. RCM processing loss for some fast and slow-time windows

than 6×10^{-2} dB for all simulations results presented in Fig. 3 and analysed in section IV-C, so only RCM processing loss effect is assessed. Three pairs of fast and slow-time windows are chosen, and simulated processing loss results are shown in solid lines in Fig. 3.

B. Asymptotic approximation of RCM processing loss

Section IV-A described the RCM processing loss obtained through simulations. An asymptotic expression for $n_{\text{RCM}} \to +\infty$ can be inferred from the roll-off rate of $-20\,\text{dB/decade}$ measured from Fig. 3.

$$\text{RCM loss (dB)} \approx -20 \log_{10} \left(n_{\text{RCM}} \text{CPL}_{\text{ft}} \text{CPL}_{\text{st}} \right) \qquad (14)$$

where CPL_{ft} and CPL_{st} are respectively the coherent processing loss (CPL) of fast and slow-time windows w_{ft} and w_{st}. The CPL of a discrete N-lengthed window w is defined as $\text{CPL} = \frac{W(0)}{N}$ [9]. The CPL represents the peak power loss of an arbitrary window against a rectangular one with the same length. A high coherent processing loss ($\text{CPL} \to 0$) mitigates the RCM processing loss at high speed, but the equivalent noise bandwidth as well as the beamwidth of the window are degraded. The SNR processing gains and frequency resolutions from the fast and slow-time windows are therefore deteriorated for severely tapered signal. The asymptotic RCM processing loss results are shown in dotted lines in Fig. 3.

C. Analysis of RCM processing loss in the automotive context

The results of simulated processing losses with 3 pairs of fast and slow-time windows are shown in Fig. 3. First, the RCM processing loss is verified when no apodization is applied on both dimensions, i.e. using rectangular windows (black solid line in Fig. 3). From simulated curves, the RCM processing loss with rectangular windows is $-1.2\,\text{dB}$ when $n_{\text{RCM}} = 1$. From Eq. (7) and modulation parameters in Table 1, one range bin of RCM corresponds to a limit speed of $V_{\text{lim}} = 56.2\,\text{km·h}^{-1}$. The $3\,\text{dB}$ loss is attained at $90\,\text{km·h}^{-1}$. When processing gain is halved (i.e. $3\,\text{dB}$ loss), the maximum detection range is reduced by $15.9\,\%$. Both radial speeds are encountered in practical automotive radar operation on the road. In the next example, slow-time only is weighted by using a Hann window (red solid line in Fig. 3). One full range bin migration induces $-0.51\,\text{dB}$ and the $3\,\text{dB}$ loss is reached at $149\,\text{km·h}^{-1}$. The use of only one window mitigates the RCM processing loss in the usual automotive speed range compared to the non-windowed case. Windowing both dimensions mitigates efficiently the phenomenon. Dolph-Chebyshev windowing is a relevant choice as the dynamic of main lobe to sidelobes is set to a targeted value while minimizing the main lobe width [9]. Weak power targets buried in the spectral leakage of more powerful targets can be detected with Dolph-Chebyshev weighting, at the expense of a degraded resolution. In the treated example, a $55\,\text{dB}$ and $50\,\text{dB}$ sidelobes attenuation are chosen in fast and slow-time respectively (blue solid line in Fig. 3), leading to a loss of $-0.26\,\text{dB}$ at $n_{\text{RCM}} = 1$ and a $3\,\text{dB}$ loss at $228\,\text{km·h}^{-1}$.

V. Conclusion

High resolution in both range and speed achieved by automotive radar results in a range cell migration, with velocities reachable in common traffic scenarios. Fast-chirp signal model relies on a decoupled range and Doppler dependency in fast and slow-time dimensions, allowing separation between range and speed estimation. A more relevant signal model includes Doppler dependency across the fast-time dimension and the pulse-to-pulse range variation in the slow-time dimension. This article shows the processing loss related to the peak spreading induced by the range migration during the CPI. Windowing the acquired sampled signal in both fast and slow-time does not influence the misestimation of the range and speed. However, the weightings penalize the most migrated ranges, which limits the smearing. The RCM processing loss expected for a pair of windows is significantly mitigated and asymptotically depends on coherent processing losses. The weighting-dependent RCM processing loss studied in this paper serves as one parameter in the radar equation, and should be compared to the others figures of merit of the windows to achieve a targeted maximum detection range.

References

[1] H. Winner, S. Hakuli, F. Lotz, and C. Singer, Eds., *Handbook of Driver Assistance Systems*. Springer International Publishing, 2016.

[2] M. Richards, *Fundamentals of Radar Signal Processing, Second Edition*. McGraw-Hill Education, 2014.

[3] H. Rohling and M. Kronauge, "Continuous waveforms for automotive radar systems," in *Waveform Design and Diversity for Advanced Radar Systems*. Institution of Engineering and Technology, Jan. 2012, 173–205.

[4] A. Bourdoux and M. Bauduin, "Near-optimal range migration and doppler ambiguity compensation for fmcw radars," in *2022 IEEE Radar Conference (RadarConf22)*, 2022, pp. 1–6.

[5] Z. Xu, C. J. Baker, and S. Pooni, "Range and doppler cell migration in wideband automotive radar," *IEEE Transactions on Vehicular Technology*, vol. 68, no. 6, pp. 5527–5536, 2019.

[6] G. Hakobyan, "Orthogonal frequency division multiplexing multiple-input multiple-output automotive radar with novel signal processing algorithms," Ph.D. dissertation, Universität Stuttgart, 2018.

[7] R. K. McCargar, J. J. Jones, G. E. Smith, and J. L. Garry, "Experimental demonstration of a highly doppler-tolerant pulsed waveform," *IEEE Transactions on Aerospace and Electronic Systems*, vol. 57, no. 6, pp. 4188–4196, 2021.

[8] D. Bok, D. O'Hagan, and P. Knott, "Effects of movement for high time-bandwidths in batched pulse compression range-doppler radar," *Sensors*, vol. 21, no. 7, 2021.

[9] K. M. M. Prabhu, *Window Functions and Their Applications in Signal Processing*. CRC Press, Sep. 2018.